RevMexAA (Serie de Conferencias), **19**, 11–22 (2003)

OPTICAL-TURBULENCE AND WIND PROFILES AT SAN PEDRO MÁRTIR

R. Avila,[1] F. Ibañez,[1] J. Vernin,[2] E. Masciadri,[3,4] L. J. Sánchez,[4] M. Azouit,[2] A. Agabi,[2] S. Cuevas,[4] and F. Garfias[4]

RESUMEN

Se presentan resultados del monitoreo de perfiles de turbulencia óptica y velocidad de las capas turbulentas en San Pedro Mártir, México. Los datos fueron colectados durante 11 noches en abril–mayo 1997 y 16 noches en mayo 2000 utilizando el Scidar Generalizado de la Universidad de Niza instalado en los telescopios de 1.5-m y 2.1-m. El análisis estadístico de los 6414 perfiles de turbulencia obtenidos muestra que la distorsión de la imagen (llamada comúnmente *seeing*) producida por la turbulencia en los primeros 1.2 km, sin incluir la turbulencia de cúpula, en los telescopios de 1.5-m y 2.1-m tiene valores medianos de 0.″63 y 0.″44, respectivamente. El *seeing* de cúpula en dichos telescopios tiene valores medianos de 0.″64 y 0.″31. La turbulencia por encima de 1.2 km y en la atmósfera completa produce *seeing* con valores medianos de 0.″38 y 0.″71. La correlación temporal de la intensidad de la turbulencia cae a 50% en períodos de tiempo de 2 y 0.5 horas, aproximadamente, para alturas mayores y menores que 16 km sobre el nivel del mar, respectivamente. La turbulencia arriba de ∼9 km permaneció notablemente débil durante 9 noches consecutivas, lo cual es alentador para realizar observaciones de alta resolución angular en el sitio. Los 3016 perfiles de la velocidad de las capas turbulentas que son analizados muestran que las capas más veloces se encuentran entre 10 y 17 km, donde se localizan la tropopausa y la corriente de chorro, con velocidad mediana de 24.4 m s^{-1}. El valor mediano del tiempo de coherencia del frente de onda es 6.5 ms, en el visible. Los resultados obtenidos en este trabajo colocan a San Pedro Mártir entre los sitios más adecuados para la instalación de telescopios ópticos de la próxima generación.

ABSTRACT

Results of monitoring optical–turbulence profiles and velocity of the turbulence layers at San Pedro Mártir, Mexico, are presented. The data were collected during 11 nights in April–May 1997 and 16 nights in May 2000 using the Generalized Scidar of Nice University installed on the 1.5–m and 2.1–m telescopes. The statistical analysis of the 6414 turbulence profiles obtained shows that the seeing produced by the turbulence in the first 1.2 km, not including dome seeing, at the 1.5–m and the 2.1–m telescopes have median values of 0.″63 and 0.″44, respectively. The dome seeing at those telescopes have median values of 0.″64 and 0.″31. The turbulence above 1.2 km and in the whole atmosphere produces seeing with median values of 0.″38 and 0.″71. The temporal correlation of the turbulence strength drops to 50% in time lags of 2 and 0.5 hours, approximately, for altitudes below and above 16 km above sea level, respectively. The turbulence above ∼9 km remained notably calm during 9 consecutive nights, which is encouraging for adaptive optics observations at the site. The 3016 profiles of the turbulent–layer velocity that are analyzed show that the fastest layers are found between 10 and 17 km, where the tropopause and the jet stream are located, with median speed of 24.4 m s^{-1}. In the first 2.2 km and above 17 km, the turbulent layers move relatively slowly, with median speeds of 2.3 and 9.2 m s^{-1}. The median of the wavefront coherence–time is 6.5 ms, in the visible. The results obtained here places San Pedro Mártir among the best suited sites for installing next generation optical telescopes.

Key Words: **ATMOSPHERIC EFFECTS — INSTRUMENTATION: ADAPTIVE OPTICS — SITE TESTING — TURBULENCE**

San Pedro Mártir: Astronomical Site Evaluation (México, D. F. and Ensenada, B. C., México, April 3-4, 2003)
Editors: Irene Cruz-González, Remy Avila & Mauricio Tapia

1. INTRODUCTION

The development and operation of ground–based modern astronomical facilities achieving high angular resolution observations, require an increasingly precise characterization of the on site atmospheric turbulence. Fundamental data for such a task are vertical profiles of the optical turbulence, represented by the refractive–index structure constant $C_N^2(h)$, and velocity of the turbulent layers $\mathbf{V}(h)$. Information about the seeing is necessary but not sufficient. For example, the design of multiconjugate adaptive optics (MCAO) (systems that incorporate several deformable mirrors, each conjugated at a dif-

[1]Centro de Radioastronomía y Astrofísica, UNAM, Morelia, México
[2]U. M. R. 6525 Astrophysique, UNSA/CNRS, France
[3]Max Plank Institut für Astronomie, Heidelberg, Germany
[4]Instituto de Astronomía, UNAM, México D.F., México

San Pedro Mártir: Astronomical Site Evaluation (México, D. F. and Ensenada, B. C., México, April 3-4, 2003)
Editors: Irene Cruz-González, Remy Avila & Mauricio Tapia

ferent altitude) requires knowledge of the statistical behavior of the optical–turbulence in the atmosphere like the altitude of the predominant turbulent layers, their temporal variability and the velocity of their displacement. Moreover, the selection of the sites where the next–generation ground–based telescopes are to be installed needs reliable studies of the C_N^2 and $\mathbf{V}$ profiles at those sites.

These reasons have motivated the accomplishment of two campaigns aimed at monitoring C_N^2 and $\mathbf{V}$ profiles at the Observatorio Astronómico Nacional de San Pedro Mártir (OAN–SPM). The campaigns took place in 1997 (April and May) and 2000 (May), for a total of 27 nights. Here we present the main results obtained from the $C_N^2(h)$ and $\mathbf{V}(h)$ measurements performed during these campaigns. Avila, Vernin, & Cuevas (1998) reported the $C_N^2(h)$ results from the 1997 observations alone. Section 2 briefly presents the measurement techniques and the observation campaigns. An overview of the monitored turbulence profiles is given in § 3 and the statistical analysis of the C_N^2 vertical distribution is presented in § 4. The temporal behavior of $C_N^2(h)$ is studied in § 5. In § 6 the wind profiles and a simple statistical analysis is presented. Finally, § 7 gives a summary of the results.

2. MEASUREMENTS OF C_N^2 AND $\mathbf{V}$ PROFILES

The principal method followed to measure the turbulence and velocity profiles at the OAN–SPM has been that of the Generalized Scidar (GS). Details of the instrumental concept, together with a complete bibliography, can be found in the web page entitled *Generalized Scidar at UNAM* [5]. Cruz et al. (2003), in this volume, present the development of a GS at UNAM. Here we give a very succinct description of the instrument and data reduction procedure. We used the GS developed by Vernin's group at Nice University (Avila, Vernin, & Masciadri 1997).

The instrumental concept for the determination of $C_N^2(h)$ consists in the measurement of the spatial autocorrelation of 1000 to 2000 double–star scintillation–images detected on a virtual plane a few kilometers below the ground. For the determination of the turbulence–layer velocity $\mathbf{V}(h)$, the cross–correlation of images delayed by 20 and 40 ms is calculated. The exposure time of each image is 1 or 2 ms and the wavelength is centered at 0.5 μm. A pair of 128×128 autocorrelation and cross–correlation maps are saved on disk every 1.2 minutes approximately. The double stars used as light sources are listed in Table 1. The data shown in this table were obtained from the Washington Double Star Catalog (Mason, Wycoff, & Hartkopf 2002). Many of the sources are multiple systems, but in every case our instrument is only sensitive to the primary and secondary components. Using a maximum entropy algorithm, one C_N^2 profile is retrieved from each autocorrelation. The data reduction of the cross–correlations is performed using an interactive algorithm (Avila, Vernin, & Sánchez 2001). In some cases, the autocorrelation and cross–correlation maps show diagonal bands parallel to each other. These are produced by video noise on the scintillation images. In such cases, the maps pass through a filter that eliminates the bands prior to do the data reduction. When the noise is still present after filtering, the maps are rejected. The vertical resolution of each C_N^2 profile depends on the star separation and the zenith angle. All the profiles were re-sampled to an altitude resolution of 500 m.

TABLE 1

DOUBLE STARS USED FOR THE GENERALIZED SCIDAR

Name	α_{2000} [a]	δ_{2000} [a]	m_1 [b]	m_2 [b]	ρ ($''$) [c]
Castor	7^h34	$31°53$	1.9	3.0	4.0
γ Leo	10^h20	$19°50$	2.3	3.6	4.5
ζ UMa	13^h24	$54°56$	2.2	3.8	14.4
δ Ser	15^h35	$10°32$	4.2	5.1	4.0
ζ CrB	15^h39	$36°38$	5.0	5.9	6.4
95 Her	18^h01	$21°36$	4.8	5.2	6.3

[a] Right ascension (α_{2000}) and Declination (δ_{2000})

[b] Visible magnitudes of each star

[c] Angular separation

2.1. *1997 Campaign*

In the 1997 observing campaign, the GS was installed on the 1.5 m and 2.1 m telescopes (1.5mT and 2.1mT) for 8 and 3 nights respectively (1997 March 23–30 and April 20–22 UT). Simultaneously, the IA–UNAM differential image motion monitor (DIMM) (Sarazin & Roddier 1990) was used to measure the open air seeing. The 2.1mT is installed on top of a 15 meter tall building lying at the summit of the mountain (2850 m above sea level) in such a way that no obstacle can generate ground turbulence. On the other hand, the 1.5mT is constructed closer to the ground level, on a site situated below the summit.

[5] http://www.astrosmo.unam.mx/~r.avila/Scidar

San Pedro Mártir: Astronomical Site Evaluation (México, D. F. and Ensenada, B. C., México, April 3-4, 2003)
Editors: Irene Cruz-González, Remy Avila & Mauricio Tapia

2.2. *2000 Campaign*

The 2000 campaign took place in May 7 through 22, UT. A number of instruments were deployed:

- **The GS**, installed during 9 and 7 nights (7–15 and 16–22 April UT) on the 1.5mT and 2.1mT telescopes, respectively.
- **Instrumented balloons**, launched to sense one detailed C_N^2 profile per night. The balloon launches require quiet wind conditions or a large area clear of obstacles in case of windy conditions. Trees and buildings of the observatory site prevented us from launching balloons when the wind was strong. In these cases, balloons were launched from Vallecitos, an area clear of trees, 3 km away from the observatory and 300 m below.
- **A 15–m–high mast**, equipped with microthermal sensors – of the same kind as those used on the balloons – to measure the C_N^2 values at 7 different altitudes up to 15 m (Sánchez et al. 2003).
- **A DIMM**, installed 8 m away from the mast, to monitor the open air seeing.
- **Meteorological balloons**, to measure the profiles of T, P, $\mathbf{V}$, and the humidity q. These were launched from Colonet, a town on the Pacific Ocean shore.

The measurements obtained with the mast and the DIMM led to a study of the contribution of the surface layer to the seeing. This work is presented by Sánchez et al. (2003) in this volume.

Most of the data gathered in this campaign were used for the calibration of the Meso–NH atmospheric model for the 3D simulation of C_N^2 (Masciadri, Avila, & Sánchez 2003).

3. $C_N^2(h)$ DATA OVERVIEW

The number of turbulence profiles measured in the 1997 and the 2000 campaigns are 3398 and 3016, making a total of 6414 estimations of $C_N^2(h)$. Figure 1 shows most of the C_N^2 profiles obtained during the 2000 campaign. The aim of that figure is to give the reader a feeling of the evolution of the turbulence profiles during each night and from night to night. The three upper rows correspond to the data obtained with the 1.5mT. In the two last rows, the data obtained with the 2.1mT is represented. The first 2.1mT night was cloudy. The blank zones correspond to either technical problems, clouds or changes of source. C_N^2 values for altitudes within the observatory and 1 km lower are to be taken as part of the response of the instrument to turbulence at the observatory level. For altitudes lower than that, the C_N^2 values are artifacts of the inversion procedure, and should be ignored.

TABLE 2

DOME SEEING STATISTICS (arcsec)

Tel.	1stQuartile	Median	3rd Quartile
1.5mT	0.55	0.64	0.77
2.1mT	0.23	0.31	0.41

Generally, the most intense turbulence is located at the observatory level, where the contributions from inside and outside of the telescope dome are added. In the statistical analysis, presented in § 4, dome turbulence is subtracted. The profiles obtained with the 2.1mT show a fairly stable and strong layer between 10 and 15 km, corresponding to the tropopause (as deduced from the balloon data). This layer is rarely present in the data obtained with the 1.5–mT. Sporadic turbulence bursts are noticed at altitudes higher than 15 km.

4. STATISTICS ON THE C_N^2 VERTICAL–DISTRIBUTION

4.1. *Dome seeing*

All the "raw" C_N^2 profiles, as those shown in Fig. 1, include in the ground layer the turbulence inside the telescope dome. For the characterization of the site, we need to remove the dome seeing contribution from the profiles. The method followed to estimate the dome C_N^2 is explained in detail by Avila et al. (2001) and some improvements are suggested by Masciadri et al. (2003). The dome seeing was determined for 84% of the profiles measured during the 2000 campaign. In the remaining 16% of the profiles, the determination of the dome seeing was "ambiguous", so we did not include these data to the dome seeing database. Refer to Avila et al. (2001) for a precise definition of an "ambiguous" determination of the dome seeing.

Figure 2 represents the cumulative distribution functions of the dome–seeing values obtained. Table 2 gives the median values, 1st and 3rd quartiles. The optical turbulence inside the 1.5mT is substantially higher than that in the 2.1mT. Note that neither cumulative distribution is symmetrical with respect to the corresponding median value.

San Pedro Mártir: Astronomical Site Evaluation (México, D. F. and Ensenada, B. C., México, April 3-4, 2003)
Editors: Irene Cruz-González, Remy Avila & Mauricio Tapia

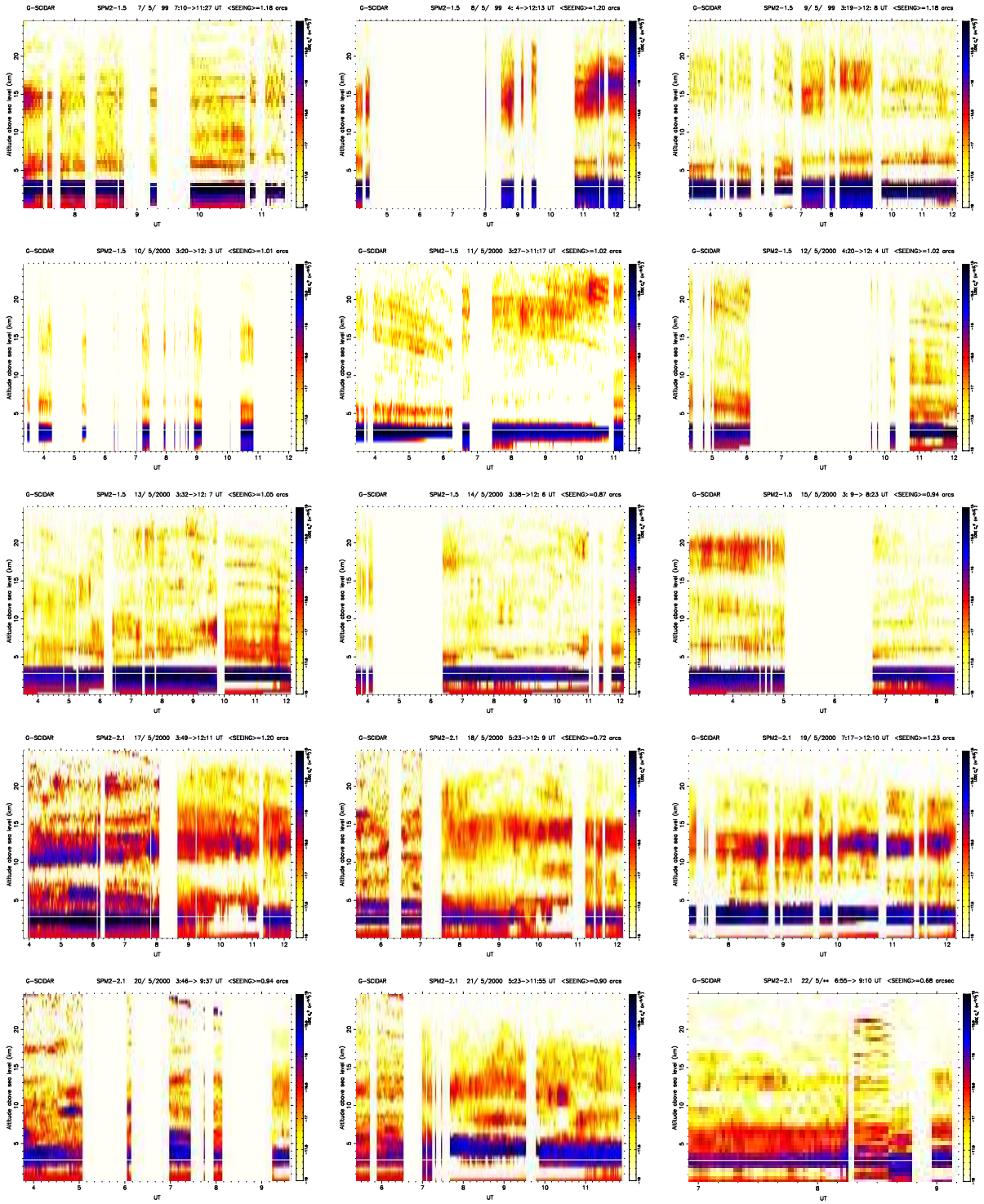

Fig. 1. Mosaic of the turbulence profiles measured during the whole campaign. Each box corresponds to one night. The vertical and horizontal axis represent the altitude (in km) above sea level and the universal time (in hours), respectively. TheC_N^2 values are coded in the color scale shown on the right–hand side of each box. The three upper rows and the two bottom rows contain the profiles obtained at the 1.5 mT and 2.1 mT, respectively. Time increases in the left–right and up–down directions. The white line centered at 2.8 km indicates the observatory altitude.

San Pedro Mártir: Astronomical Site Evaluation (México, D. F. and Ensenada, B. C., México, April 3-4, 2003)
Editors: Irene Cruz-González, Remy Avila & Mauricio Tapia

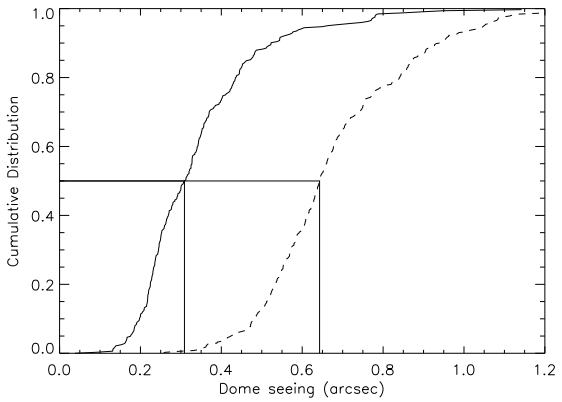

Fig. 2. Cumulative distribution of the seeing generated inside the dome of the 2.1mT (full line) and the 1.5mT (dashed line). The vertical and horizontal lines indicate the median values. These values together with the 1st and third quartiles are reported in Table 2.

In the remaining part of the paper, all the statistical results concerning the turbulence near the ground are free of dome–turbulence.

4.2. *Median profiles*

The median, 1st and 3rd quartiles values of $C_N^2(h)$ obtained with the 1.5mT and 2.1mT are represented in Figs. 3a and 3b respectively. These profiles were computed using the data from both campaigns, i.e. the complete GS data set, with the dome seeing removed. The most important characteristic is that the turbulence measured at the telescope level is notably more intense at the 1.5mT than at the 2.1mT. We believe that this is principally due to the fact that the 1.5mT is located at ground level, while the 2.1mT is installed on top of a 20–m building. Moreover, the 2.1mT building is situated at the observatory summit whereas the 1.5mT is located at a lower altitude. Figure 3c shows the median profile calculated from all the C_N^2 profiles measured with the GS in the OAN–SPM (i.e. both campaigns).

Another difference seen in the median profiles obtained with the 1.5mT and 2.1mT (Figs. 3a and 3b) is that the tropopause layer, which is centered at 12 km approximately, is much stronger on Fig. 3b than on Fig. 3a. This is not a consequence of the telescope which was used. By chance, it happened that while observing with the 1.5mT during the 2000 campaign the turbulence at that altitude – and everywhere higher than 8 km – was very weak, as seen on Fig. 4. During that campaign, between the 1.5mT and 2.1mT observations, there was one cloudy night. In contrast with the first 9 nights of the campaign

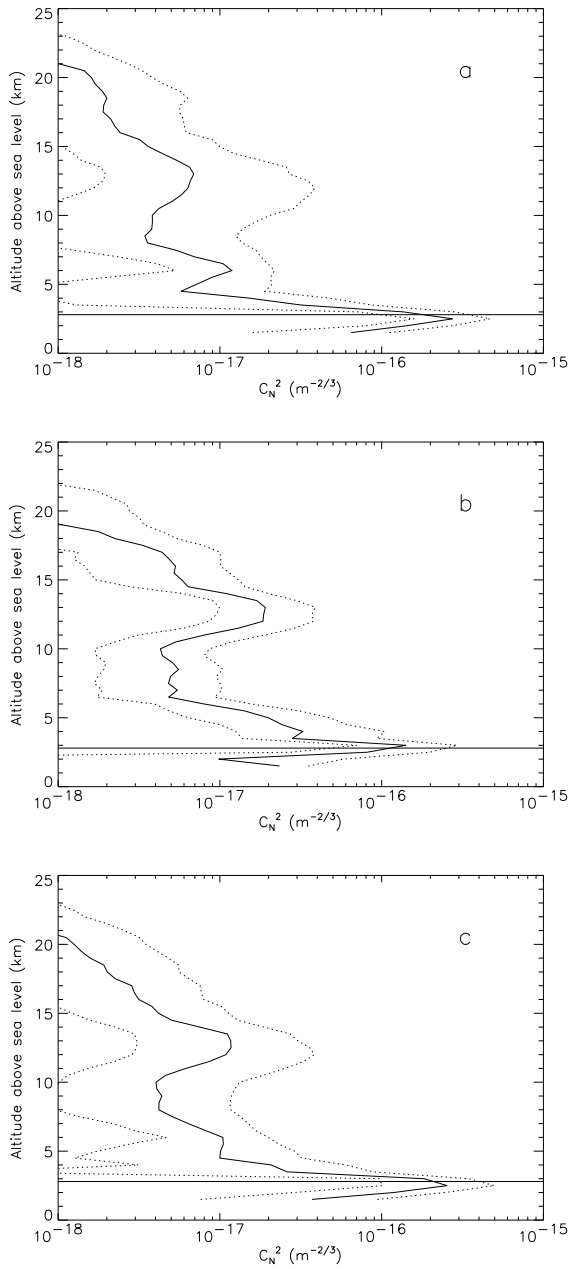

Fig. 3. Median (full line), 1st and 3rd quartiles(dashed lines) of the $C_N^2(h)$ values obtained with the GS at the (a) 1.5mT , (b) 2.1mT and (c) both telescopes, during 1997 and 2000 campaigns. The horizontal axis represents C_N^2 values, in logarithmic scale, and the vertical axis represents the altitude above sea level. The horizontal lines indicate the observatory altitude. Dome seeing has been removed.

San Pedro Mártir: Astronomical Site Evaluation (México, D. F. and Ensenada, B. C., México, April 3-4, 2003)
Editors: Irene Cruz-González, Remy Avila & Mauricio Tapia

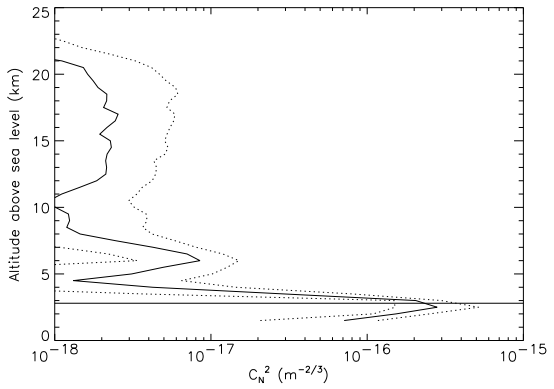

Fig. 4. Similar to Fig. 3 but for the GS profiles obtained at the 1.5mT during the 2000 campaign.

(when the GS was installed on the 1.5mT), during the first observable night on the 2.1mT, the turbulence in the tropopause was extremely intense. This can be seen on the first box of the 4th row of Fig. 1. It is generally believed that the turbulence intensity at the tropopause is strong due to a dramatic increase of the overall vertical gradient of the potential temperature and the commonly high–velocity wind (jet stream) in that zone of the atmosphere. However, new evidence that contradicts this speculation – or at least that suggests a more complicated phenomenon – is emerging, which motivates a deeper investigation. A first step could be to gather a more complete statistical data set. For the moment, we note that 32% of the profiles measured at the OAN–SPM do not show a significant optical turbulence at the tropopause.

4.3. *Seeing for different atmospheric slabs*

From a visual examination of Fig. 1, we can determine five altitude slabs that contain the predominant turbulent layers. These are [2;4], [4;9], [9;16], [16;21] and [21;25] km above sea level. In each altitude interval of the form $[h_l;h_u]$ (where the subscripts l and u stand for "lower" and "upper" limits) and for each profile, we calculate the turbulence factor

$$J_{h_l;h_u} = \int_{h_l}^{h_u} \mathrm{dh}\ \mathrm{C_N^2(h)}, \qquad (1)$$

and the correspondent seeing in arc seconds:

$$\epsilon_{h_l;h_u} = 1.08 \times 10^6 \lambda^{-1/5} J_{h_l;h_u}^{3/5}. \qquad (2)$$

For the turbulence factor corresponding to the ground layer, $J_{2;4}$, the integral begins at 2 km in order to include the complete C_N^2 peak that is due to

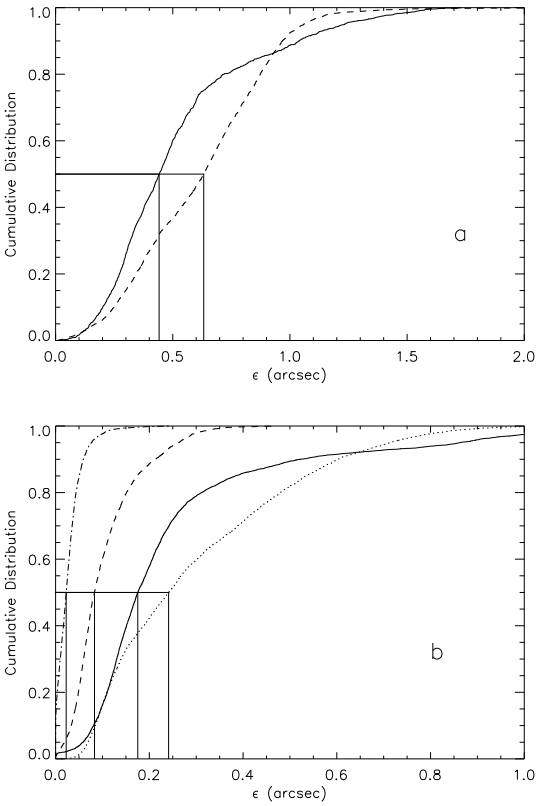

Fig. 5. Cumulative distributions of the seeing generated in different atmosphere slabs: (a) [2;4] km for the 2.1mT (full line) and the 1.5mT (dashed line) without dome seeing; (b) [4;9] km (full line), [9;16] km (dotted line), [16;21] km (dashed line), [21;25] km (dash–dotted line). The horizontal and vertical lines indicate the median values, which are reported in Table 3.

turbulence at ground level (2.8 km). Moreover, $J_{2;4}$ does not include dome turbulence. The seeing values have been calculated for $\lambda = 0.5$ μm. In Fig. 5a the cumulative distribution functions of $\epsilon_{2;4}$ obtained at the 1.5mT and the 2.1mT, calculated using the complete data set, are shown. As discussed in § 4.2, the turbulence at ground level at the 1.5mT is higher than that at the 2.1mT. The cumulative distributions of the seeing originated in the four slabs of the free atmosphere (from 4 to 25 km) are represented in Fig. 5b. The strongest turbulence is encountered from 9 to 16 km, where the tropopause layer is located. The turbulence at altitudes higher than 16 km is fairly weak, which is a fortunate feature for the use of adaptive optics, because it tends to increase the corrected field–of–view. Finally, Figs. 6a and 6b show the cumulative distribution of the seeing produced in the free atmosphere, $\epsilon_{4;25}$, and in the whole

San Pedro Mártir: Astronomical Site Evaluation (México, D. F. and Ensenada, B. C., México, April 3-4, 2003)
Editors: Irene Cruz-González, Remy Avila & Mauricio Tapia

TABLE 3

SEEING STATISTICS FOR DIFFERENT ATMOSPHERE SLABS (arcsec)

Slab (km)	1st Q[a]	Median	3rd Q[a]
[2; 4] @ 2.1mT[b]	0.30	0.44	0.63
[2; 4] @ 1.5mT[b]	0.38	0.63	0.83
[4; 9]	0.12	0.17	0.27
[9; 16]	0.12	0.24	0.43
[16; 21]	0.05	0.08	0.14
[21; 25]	0.01	0.02	0.04
[2; 25][c]	0.52	0.71	0.99

[a]1st and 3rd quartiles

[b]Without dome seeing

[c]As if measured at the 2.1mT and without dome seeing (see text)

atmosphere, $\epsilon_{2;25}$, respectively. The computation of $\epsilon_{2;25}$ is performed as follows: for each profile of the complete data set (both campaigns and both telescopes) we calculate $J_{4;25}$ and add a random number that follows the same log–normal distribution as that of $J_{2;4}$ obtained in for the 2.1mT. Then the corresponding seeing value is calculated using Eq. 2. This way, we obtain a distribution of $\epsilon_{2;25}$ values as if they were measured using the 2.1mT. The reason for doing so, is that the values of $\epsilon_{2;25}$ that we obtain are more representative of the potentialities of the site than if we had used the distribution of $J_{2;4}$ obtained for the 1.5mT. The median values of all the cumulative distributions presented in this Section are reported in Table 3.

5. TEMPORAL AUTOCORRELATION

What are the characteristic temporal scales of the fluctuations of optical turbulence at different altitudes in the atmosphere? This question has been of interest for a long time, and mostly in recent years, as the development of Multiconjugate Adaptive Optics (MCAO) require knowledge of the properties of the optical turbulence in a number of slabs in the atmosphere. Racine (1996) studied the temporal fluctuations of free atmosphere seeing above Mauna Kea. He computed the seeing values by integrating turbulence profiles measured in 1987 by Vernin's group from Nice University using the scidar technique. The C_N^2 profiles did not include the turbulence from the first kilometer, because the classical mode of the scidar was employed, as the generalized mode did not exist at that time. Muñoz-Tuñón, Varela, & Vernin (1992) used DIMM data to study the temporal behavior of the open–air seeing at Roque de Los Muchachos observatory. Finally, Tokovinin, Baumont, & Vasquez (2003) presented the temporal autocorrelation of the turbulence factor in three representative slabs of the atmosphere above Cerro Tololo Interamerican Observatory, using data obtained with the recently developed Multi–Aperture Scintillation Sensor, which provides C_N^2 measurements at six altitudes in the atmosphere.

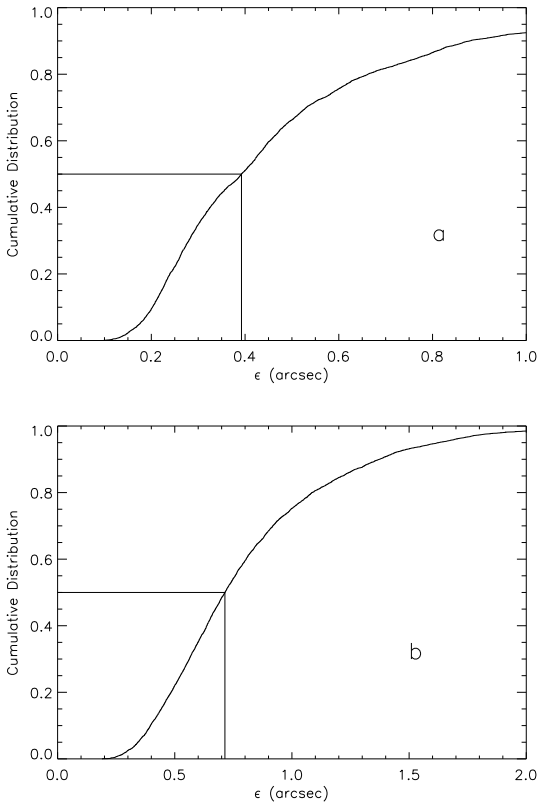

Fig. 6. Cumulative distributions of the seeing generated in (a) the free atmosphere (altitude higher than 4 km) and (b) the whole atmosphere, without dome seeing (see text for details). The horizontal and vertical lines indicate the median values, which are reported in Table 3.

In this Section we investigate the temporal autocorrelation of the turbulence factors $J_{h_l;h_u}$, for the five slabs introduced in § 4.3.

5.1. *Methodology*

The process of building the appropriate sequences of $J_{h_l;h_u}(t_i)$ values is explained below:
Typically, three stars are used as light sources each night, in a sequence such that the zenith angle never exceeds ∼40°. When changing from one star to the

San Pedro Mártir: Astronomical Site Evaluation (México, D. F. and Ensenada, B. C., México, April 3-4, 2003)
Editors: Irene Cruz-González, Remy Avila & Mauricio Tapia

following, the region of the atmosphere that is sensed by the instrument changes significantly and so $C_N^2(h)$ can also change, as shown by Masciadri, Avila, & Sánchez (2002). To avoid the confusion between a temporal and a spatial variation of $J_{h_l;h_u}$, the sequences $J_{h_l;h_u}(t_i)$ never include data obtained with two different stars. From the 2000–campaign data, we built 35 sequences $J_{h_l;h_u}(t_i)$ for each of the five altitude intervals. The temporal sampling of the turbulence profiles depends on the number of scintillation images recorded for the computation of each profile, which in turn depends on the source magnitude. Consequently, each sequence $J_{h_l;h_u}(t_i)$ is resampled with a regular time–interval of $\delta t = 1.14$ minutes, which is the mean temporal sampling of the C_N^2 profiles. Moreover, while observing a given source, the data acquisition may be interrupted. If the interruption is longer than $2\delta t$, then the temporal gap is filled with zero values for $J_{h_l;h_u}(t_i)$.

For each altitude interval, the calculation of the temporal autocorrelation, as a function of the temporal lag Δt, is performed as follows: For each $J_{h_l;h_u}$ sequence labeled s, we first compute

$$C_s(\Delta t) = \sum_{i=1}^{N_{\Delta t,s}} \left(J_s(t_i) - \overline{J_s}\right)\left(J_s(t_i+\Delta t) - \overline{J_s}\right), \tag{3}$$

where the product is set equal to zero if either $J_s(t_i) = 0$ or $J_s(t_i + \Delta t) = 0$. $\overline{J_s}$ is the mean of the nonzero values of $J_s(t_i)$, and $N_{\Delta t,s}$ is the number of computed nonzero products, which depends on Δt and the number of nonzero values of $J_s(t_i)$ in the sequence s, and is calculated numerically. The autocorrelation for each altitude slab is then given by

$$\Gamma(\Delta t) = \frac{A(\Delta t)}{B}, \text{ where} \tag{4}$$

$$A(\Delta t) = \frac{1}{N_{\Delta t}} \sum_{s=1}^{N_s} C_s(\Delta t), \tag{5}$$

$$B = \frac{1}{N_0} \sum_{s=1}^{N_s} C_s(0) \text{ and} \tag{6}$$

$$N_{\Delta t} = \sum_{s=1}^{N_s} N_{\Delta t,s}. \tag{7}$$

N_s is the number of sequences for each altitude interval. From the definitions of $C_s(\Delta t)$ and $N_{\Delta t}$ (Eqs. 3 and 7), it can be noticed that the normalization factor B only takes into account nonzero values of $J_s(t_i)$.

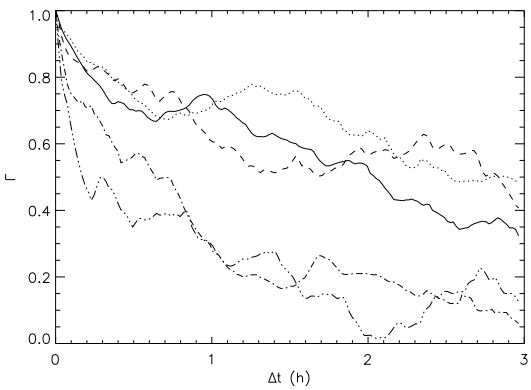

Fig. 7. Temporal autocorrelation of the turbulence factor $J_{h_l;h_u}(t_i)$, for intervals $[h_l;h_u]$ equal to [2;4] (full line), [4;9] (dotted line), [9;16] (dashed line), [16;21] (dash–dotted line) and [21;25] (dash–dot–dotted line) km.

5.2. *Results*

The temporal autocorrelations for the five atmosphere slabs were computed using the 2000–campaign data set. The turbulence inside the dome was removed. The number $N_{\Delta t}$ of products summed to calculate $\Gamma(\Delta t)$ range from ∼2902 for $\Delta t = 0$ to ∼870 for $\Delta t = 3$ hrs. The results are shown in Fig. 7. For every slab, the autocorrelation shows a steep descent for short temporal lags followed by a less rapid decrease for longer lags. It can be seen that in the first three altitude slabs the turbulence de-correlate more slowly than in the two higher slabs. The time lags for a 50% decorrelation are approximately 2, 2.5, 1.7, 0.7 and 0.2 hours in the altitude ranges [2;4], [4;9], [9;16], [16;21] and [21;25] km, respectively. The turbulence in the highest slab is so weak (as seen in Fig. 5), that $\Gamma(\Delta t)$ for that slab might be strongly affected by the noise variations. Turbulence in the highest layers evolve more rapidly than in the lower layers but introduces less distortions in the wavefront because they are weaker. In the altitude rages [2;4] and [9;16] km the turbulence is the most intense, but fortunately, the variations are slow.

6. WIND PROFILES

We present the wind profiles obtained in the 2000 campaign. Each of the 3016 C_N^2 profile of that campaign has an associated **V** profile. Fig. 8 shows a mosaic view of all the wind–speed profiles obtained during the campaign, similarly to the C_N^2 profiles shown in Fig. 1. It can be seen that at the observatory level, the wind is generally extremely weak. At

San Pedro Mártir: Astronomical Site Evaluation (México, D. F. and Ensenada, B. C., México, April 3-4, 2003)
Editors: Irene Cruz-González, Remy Avila & Mauricio Tapia

that altitude, the figures show the speed of the turbulence inside the telescope dome, which is zero, and outside the dome, where the wind is generally slow but higher than zero. In many cases, dots with different colors appear superimposed, which indicates the presence of several turbulent layers with altitude differences smaller than the vertical resolution of the C_N^2 profiles, but with velocity differences that are detectable. The fastest turbulent layers are found between 9 and 16 km. In this altitude range, where the jet stream is located, the wind speed reaches 20 m s^{-1} only during 7 out of 15 nights. On 2000, May 17 UT (4th row, 1st column in Fig. 1), the wind at that altitude range reached 55 m s^{-1} and was stronger than 20 m s^{-1} all along the night. For altitudes higher than 16 km, the wind intensity begins to decrease and above 20 km it is extremely slow. From a visual inspection of Figs. 1 and 8, it can be seen that only the night on 2000, May 17 UT and in the jet stream layer, an evident correlation is present between the C_N^2 and $\mathbf{V}$ values. The histograms of the speed values in the altitude ranges [2;5], [5;10], [10; 17] and [17; 25] km are represented in Fig. 9. The peak at 0 m s^{-1} in Fig. 9a is due to the turbulence inside the dome. The median values in the above mentioned regions of the atmosphere are 2.3 , 11.3, 24.4 and 9.2 m s^{-1}, respectively.

From each pair of C_N^2 and $\mathbf{V}$ profiles, one can compute the wavefront coherence–time τ_0. The expression given by Roddier, Gilli, & Lund (1982):

$$\tau_0 = 0.519 \left(\frac{2\pi}{\lambda}\right)^{-5/6} \left[\int \mathrm{d}h |\mathbf{V}(h)|^{5/3} C_N^2(h)\right]^{-3/5} \quad (8)$$

corresponds to the coherence time for an ideal full–correction adaptive optics system. The median of the τ_0 values computed from the 3014 $C_N^2(h)$ and $\mathbf{V}(h)$ pairs available is 6.5 ms for $\lambda = 0.5$ μm. Masciadri & Garfias (2002) made a study of τ_0 using C_N^2 profiles simulated with the Meso–NH atmospheric model, finding similar τ_0 values in the summer period as those found here.

7. SUMMARY AND CONCLUSIONS

Turbulence profiles and velocity of the turbulence layers have been monitored at the OAN–SPM, during 11 nights in April–May 1997 and 16 nights in May 2000. The GS was installed at the foci of the 1.5mT and 2.1mT. Turbulence inside the dome is detected by the instrument, but for each profile, this contribution has been estimated and separated from the turbulence near the ground outside the dome. The result is a data set consisting of two subsets: turbulence profiles free of dome seeing and dome seeing values. The statistical analysis of this data set lets us draw the following conclusions:

- The turbulence inside the 1.5mT is much stronger than that at the 2.1mT, with median values of 0.″64 and 0.″31.
- The precise location of each telescope influences the turbulence measured near the ground. The 1.5mT is installed basically at ground level and lower than the site summit, while the 2.1mT is on top of a 20–m building and at the site summit. A consequence of this is that the median values of the seeing produced in the first 1.2 km are 0.″63 and 0.″44 for the 1.5mT and 2.1mT, respectively.
- The seeing generated in the free atmosphere (above 1.2 km from the site), has a median value of 0.″38. This very low value encourages adaptive optics observations, as the lower the turbulence in the higher layers, the broader is the corrected field of view.
- The seeing in the whole atmosphere without the dome contribution as measured from the 2.1mT, has a median value of 0.″71.
- The temporal autocorrelation of the turbulence factors $J_{h_l;h_u}$ (see § 4.3) shows that C_N^2 evolves sensibly more slowly in the layers below 16 km (above see level) than in the layers above that altitude. The time lag corresponding to a 50% decorrelation is approximately equal to 2 and 0.5 hours for turbulence below and above 16 km, respectively. The longer the decorrelation time, the higher the potential performances of adaptive–optics observations are and the easier would be the development of multiconjugate adaptive optics systems. Rapid evolution of the C_N^2 in the highest layers is in principle a negative behavior. However, this is counterbalanced by the very low C_N^2 values in those layers. Further investigations will include the temporal correlation of the isoplanatic angle, which would integrate both effects.

From the GS data obtained during the 2000 campaign, a statistical analysis of the velocity of the turbulence layers has been made. The principal results and conclusions are the following:

- No evident general correlation between the C_N^2 value in a layer and the layer speed has been found. The correlation is only evident during

San Pedro Mártir: Astronomical Site Evaluation (México, D. F. and Ensenada, B. C., México, April 3-4, 2003)
Editors: Irene Cruz-González, Remy Avila & Mauricio Tapia

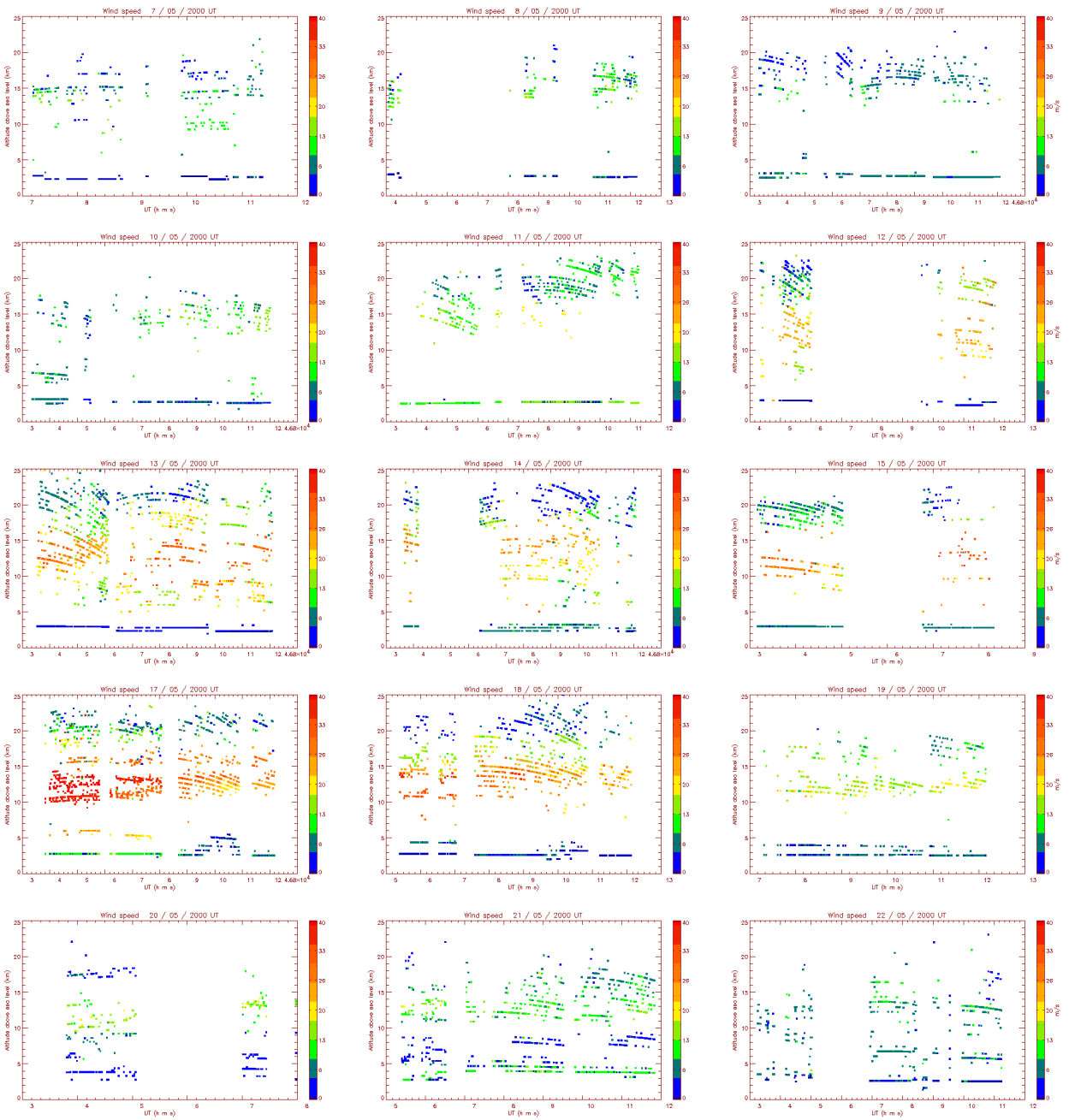

Fig. 8. Similar to Fig. 1, but the colors represent wind speed. Each dot indicates one turbulent layer.

one night, in which C_N^2 and **V** values around 12 km are extremely high. This fact might indicate that only for **V** values higher than a certain threshold level, the C_N^2 value is correlated to the **V** value. Further investigation is needed to prove or disprove this conjecture.

- The fastest layers are found between 10 and 17 km, with median speed value of 24.4 m s^{-1}. The layers above 17 km go notably more slowly (median speed of 9.2 m s^{-1}), which is a positive feature for adaptive optics, because the wavefront deformations introduced by those layers would be corrected to a better degree than the lower layers, resulting in a wider field of view.

- The wavefront coherence–time for an ideal full–correction adaptive optics system has a median

San Pedro Mártir: Astronomical Site Evaluation (México, D. F. and Ensenada, B. C., México, April 3-4, 2003)
Editors: Irene Cruz-González, Remy Avila & Mauricio Tapia

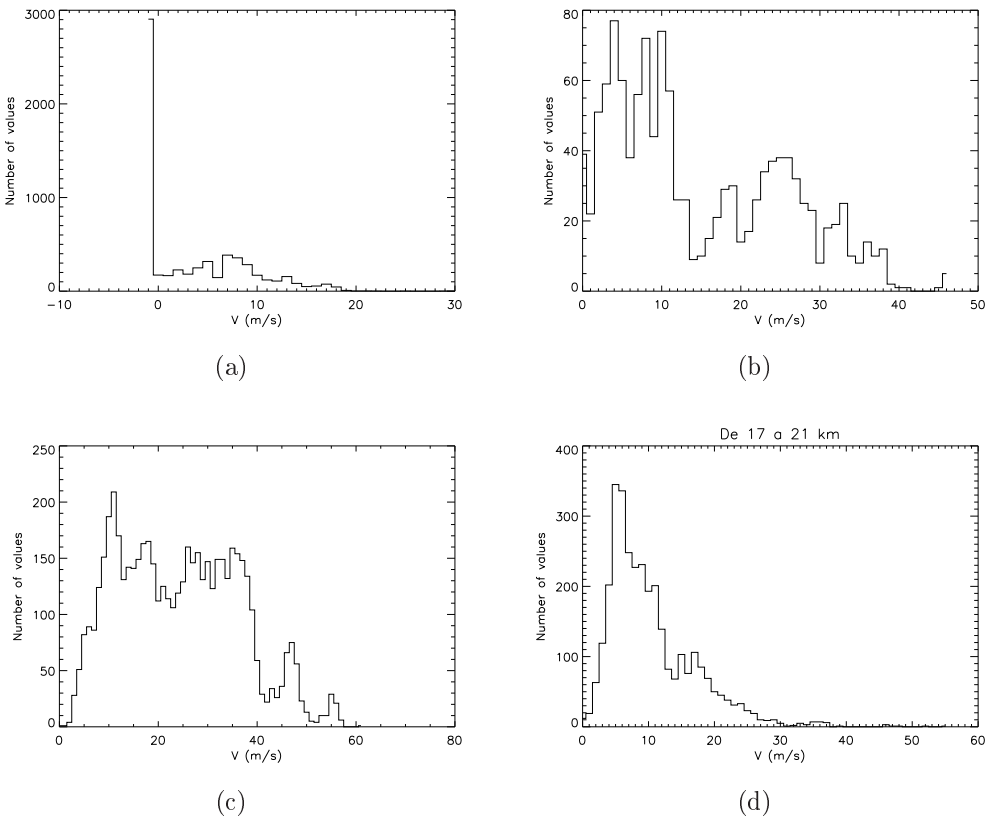

Fig. 9. Histograms of the wind–speed values at the altitude intervals (a) [2;5], (b) [5;10], (c) [10; 17] and (d) [17; 25] km.

value of 6.5 ms.

Of particular interest are studies of the potential performances of multiconjugate adaptive optics systems for Extremely Large Telescopes (ELT). These studies can be carried out with the data set of paired C_N^2 and **V** profiles. For example, one can optimize the number of actuators and the temporal frequency of the different deformable mirrors for a required size of the corrected field of view. From the results obtained in this work, a qualitative guess is that a deformable mirror conjugated at 12 km would need less actuators but be faster than a deformable mirror conjugated at ground level.

The C_N^2 and **V** profiles are extremely important for the choice of the site for an ELT or any optical telescope with adaptive optics. The studies performed at the OAN–SPM have revealed that the site has truly excellent turbulence conditions. However, a longer–term monitoring is desirable, in order to confirm our results and identify seasonal behaviors, which is the motivation of developing a GS at UNAM.

We are grateful to the OAN–SPM staff for their valuable support. This work was done in the framework of a collaboration between the Instituto de Astronomía of the Universidad Nacional Autónoma de México and the UMR 6525 Astrophysique, Université de Nice–Sophia Antipolis (France), supported by ECOS–ANUIES grant M97U01. Funding was also provided by the grants J32412E from CONACyT, IN118199 from DGAPA–UNAM, and the TIM project (IA-UNAM).

REFERENCES

Avila, R., Vernin, J., & Cuevas, S. 1998, PASP, 110, 1106
Avila, R., Vernin, J., & Masciadri, E. 1997, Appl. Opt., 36, 7898
Avila, R., Vernin, J., & Sánchez, L. 2001, A&A, 369, 364
Cruz, D. X., et al. 2003, RevMexAA(SC) 19,44
Masciadri, E., Avila, R., & Sánchez, L. 2002, A&A, 382, 378
Masciadri, E., Avila, R., & Sánchez, L. 2003, RevMexAA, *submitted*
Masciadri, E., & Garfias, T. 2002, A&A, 366, 708
Mason, B., Wycoff, G., & Hartkopf, W. I. 2002,

http://ad.usno.navy.mil/wds
Muñoz-Tuñón, C., Varela, A., & Vernin, J. 1992, A&AS, 125, 183
Racine, R. 1996, PASP, 108, 372
Roddier, F., Gilli, J., & Lund, G. 1982, J.Opt. (Paris), 13,263
Sánchez, L., et al. 2003, RevMexAA(SC) 19,23
Sarazin, M., & Roddier, F. 1990, A&A, 227, 294
Tokovinin, A., Baumont, S., & Vasquez, J. 2003, MNRAS, 340, 52

San Pedro Mártir: Astronomical Site Evaluation (México, D. F. and Ensenada, B. C., México, April 3-4, 2003)
Editors: Irene Cruz-González, Remy Avila & Mauricio Tapia

Abdelkrim Agabi, Max Azouit and Jean Vernin: U. M. R. 6525 Astrophysique, Université de Nice Sophia Antipolis/CNRS, Parc Valrose, 06108 Nice Cedex 2, France (karim.agabi,max.azouit,jean.vernin@unice.fr).
Remy Avila, Fabiola Ibañez: Centro de Radioastronomía y Astrofísica, Universidad Nacional Autónoma de México, Campus Morelia, Apartado Postal 3–72, 58090 Morelia, Michoacán, México (r.avila@astrosmo.unam.mx).
Salvador Cuevas, Fernando Garfias and Leonardo J. Sánchez: Instituto de Astronomía UNAM, Apdo. Postal 70–264, 04510 México D.F., México (chavoc,fergar,leonardo@astroscu.unam.mx).
Elena Masciadri: Max Planck Institut für Astronomie, Königstuhl 17, D–69117 Heidelberg, Germany (masciadri@mpia.de).